



Reactive PLD of ZnO thin film for optoelectronic application

Evan T. Salem¹ Raid A. Ismail² Makaram A. Fakhry^{3*} Yushamdan Yusof⁴

1 University of Technology, Baghdad, Iraq

2 Institute of Nano Electronic Engineering (INEE), University Malaysia Perlis (UniMAP), Perlis, Malaysia

3 Laser and Optoelectronic department, University of technology, Baghdad, Iraq*

4 University science Malaysia

Received 11 April 2015; Revised 29 June 2015; Accepted 13 July 2015

Abstract

ZnO/Si heterostructure has been constructed on (111) oriented silicon substrate using a pulsed Nd: YAG laser for the ablation of Zn target in the presence of oxygen as reactive atmosphere in order to prepare ZnO TCO's films. Were the electrical properties of these films have been invested reaching to the optimum oxygen pressure at which the device has been prepared. ZnO films, formed at 300 Torr oxygen ambient, showed an electrical resistivity of 0.27 Ω .cm, without using post-deposition heat treatment. The electrical properties of the preparation device have been carried out at different substrate temperatures. Also the detector parameter has been measured

Keywords: TCO thin film; MIS device; PLD deposition; electrical properties.

PACS: 71.20.Nr; 74.78._w; 73.40.Lq; 73.50.Pz.

1. Introduction

Transparent Conducting Oxide (TCO) film is an electrically conductive material that is highly transparent in the range of visible wavelengths as well as electrically conductive [1-4]. The importance of this material can be traced back to the 20th century, when the first films were recorded with their unique properties[5-7]. This material has found extensive applications in optoelectronic devices such as solar cells, Liquid Crystal Display (LCD), heat mirrors and many other different applications depending on the type of material [8-12]. The aim of many manufacturers, beyond the fabrication of TCO films, is to achieve stable properties for large area coating processes with low film resistance and high transmittance within the visible region of the electromagnetic spectrum. The simultaneous occurrence of high optical transparency in the visible region and high electrical conductivity is not possible with intrinsic stoichiometries materials, but partial transparency and possibly good conductivity may be obtained in thin films of a variety of metals. The only way to obtain good transparent conductors is to create electron degeneracy in a wide band gap (3eV) oxide by controllably introducing non - stoichiometry and/or appropriate dopants [13,14]. With the use of oxygen or nitrogen gas, it is possible to produce oxides' or nitride dielectric layers from metal targets [5]. The optoelectronic of ZnO thin films depend on the

deposition and post-deposition treatment conditions as these properties change significantly with [15,16]

1. The nature of choosing doping element
2. The adsorption of oxygen that takes place during film deposition
3. Film deposition temperature
4. Description during annealing treatment in a ready atmosphere

The wide band gap of this material makes it an excellent visible light transparent and the UV absorbing material. This, together with its low toxic effect, makes it an ideal material to use in sunscreen as a UV blocking element. Depending on the deposition conditions (substrate temperature and oxygen pressure), the ZnO films can be divided into three groups, the first group belongs to a mixture of ZnO and metallic zinc; and these films are conductive and opaque, the second group of films has a composition close to stoichiometric bulk ZnO; they are non-conductive but transparent, while films of the third group are of high importance in optoelectronic applications since they are transparent and conductive films[17].

In the last ten years a lot of work could be found in the field of laser ablation of ZnO nanostructure, M.Bouderbala et al, investigate the effect of film thickness upon their structural, morphological, electrical and optical properties. The results suggest that the film thickness seems to have no clear effect upon the orientation of the grains growth.[18] Inorganic nano-crystallites such as (CdO, ZnO, ZnS, ZnSe) were incorporated into photopolymer matrices (7.5% by weight) and optically treated with coherent bicolor nanosecond laser pulses at Er³⁺ glass laser lines at 1.54 and 0.77 μm . They have achieved a sufficiently good effective second-order susceptibility coefficients (up to 2.8 pm/V) at wavelengths 1.54 μm . The maximal second-order optical susceptibility was achieved for NC sizes equal to about 30 nm^[19]. For the same nanomaterial a theoretical study was done on the structural, optical and electronic properties of ZnO nano structure [20]

In this work effect of O₂ pressure on ZnO film properties were studied in order to find optimum preparation condition, at which optoelectronic device was prepared and characterized.

2. Experiment

Undoped ZnO thin films were deposited on cleaning glass substrates by using pulsed Nd:YAG laser deposition technique, Fig. 1 shows the schematic diagram of PLD system used in this study.

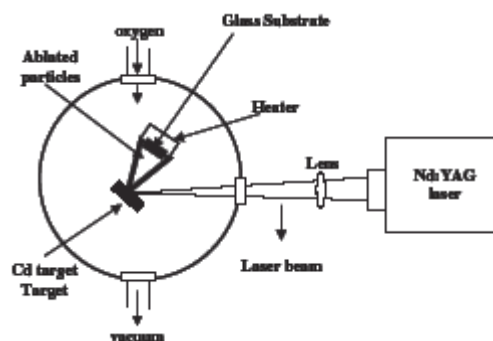


Fig. 1: schematic diagram PLD system

Pulses of Q- switched Nd:YAG laser with 30 ns (FWHM) and $\lambda = 1.064 \mu\text{m}$ were focused through 20 cm focal length of converging lens onto a high purity cadmium target (99.999% provided from Fluka com.) at 45° angle of incidence. The target rotated with a frequency of 10 Hz. The pulse energy density of laser at the target surface was maintained at 2 J/cm^2 . All films were produced using 30 laser shots and deposited at a substrate temperature of 250°C (this growth temperature was Optimum [21] in background oxygen pressure ranged from 50-350 Torr for preparing ZnO. The film thickness was measured by a stylus profilometer. The sheet resistance and conductivity type of these films were determined using four point probe (FPP 5000). After that (111) crystalline Si substrate has been used for device preparation. Electrical, photovoltaic properties at different substrate temperature has been carried out.

3. Results and discussion

The relation between the logarithmic conductivity as a function of temperature of the samples prepared at different O₂ pressures and the optimum substrate temperature is given in figure 2.

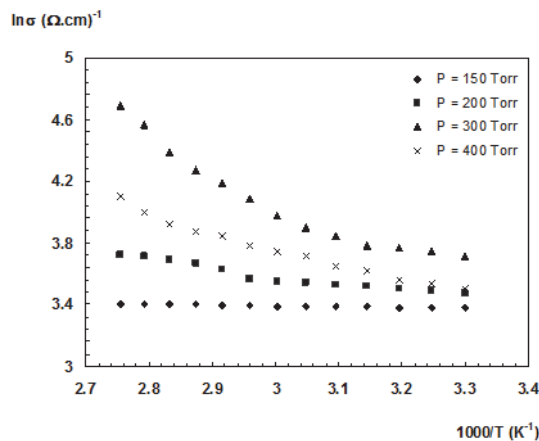


Fig. 2: Electrical conductivity vs. $1000/T$ at different O₂ pressure for Zn target

For samples at low temperature region and at low pressure, the slope of the curve tends to be zero due to the presence of Fermi level in the conduction band of such degenerated material. Increasing the O₂ pressure further, the sample transforms gradually to be a semiconductor. The linear proportionality in the second part of the curve is related to the increase in the number of ionized carriers from the conduction band to the valence band as the substrate is heated. The conduction characteristics of oxide films are primarily dominated by electrons generated due to the O⁻² vacancies and metallic interstitial atoms. It has been found that the resistivity of TCO material increases with the deviation from the non-stoichiometry to stoichiometry as this deviation will drive less O₂ vacancies and hence little electron concentration in the conduction band.

For this reason, the value of the resistivity (ρ) increases as shown in figure 3 and carrier concentration (n) decreases as shown in figure 4 at high oxygen pressure (>300 torr), These values of O₂ pressure were found to be the optimum.

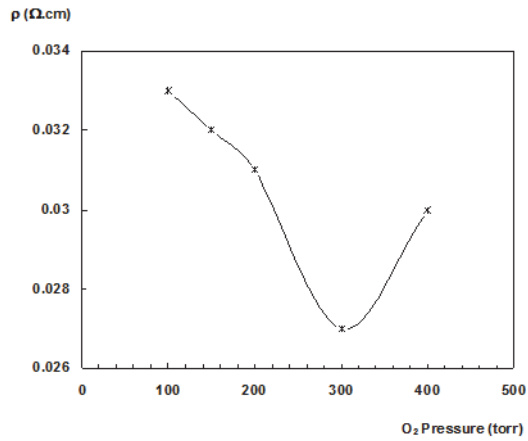


Fig. 3: Resistivity vs. O₂ pressure for Zn samples

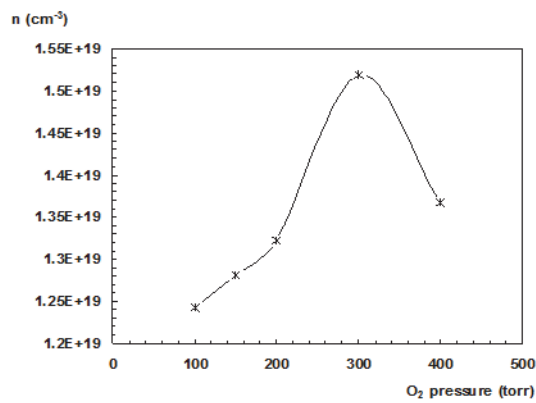


Fig. 4: Carrier concentration vs. O₂ pressure for ZnO samples

The conductivity type of the prepared semiconductor films is introduced by measuring Seebeck coefficient and figure 5 gives the relation between thermo-electric power and the heating temperature for samples prepared at optimum O₂ pressure and substrate temperature.

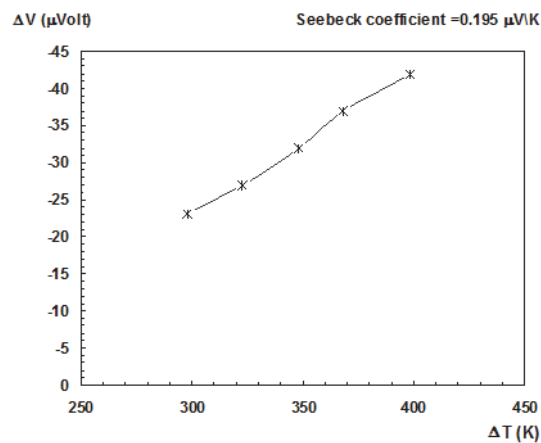


Fig. 5: Thermoelectric power as a function of heating temperature for ZnO, the values of Seebeck coefficient are 0.195 μV/K

The results indicate that the studied materials are thought to be n-type semiconductor possibly due to the donor formation by O₂ vacancies and interstitial metal atoms, These results is agreeing with published literatures^[22] An optimization between the electrical

conductivity and optical transparency could be obtained from the value of the figure of merit (F.M.) shown in figure 6 as a function of O₂ pressure.

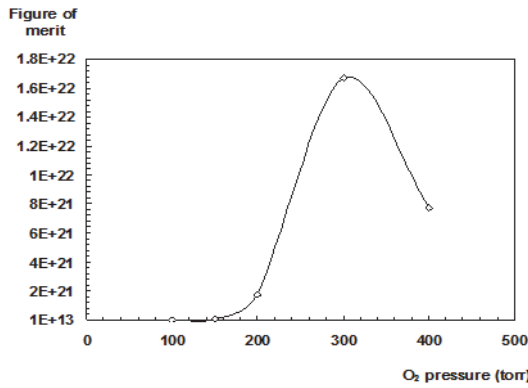


Fig. 6: Figure of Merit vs. O₂ pressure for ZnO samples

At low O₂ pressure, the metallic films have very low transparency and very high conductivity due to metallic properties. As a result, low F.M. value would achieve with further increase the film transparency and decrease conductivity. This behavior keeps up to the optimum O₂ pressure where the ratio between the metal atoms and the oxide atoms is equal to (60/40)% and the material is fully non-stoichiometry as explained in chapter one. Further increase in O₂ pressure (400torr), the value of F.M. decreases due to the non stoichiometries conversion of the material leading to reduced electrical conductivity, while the optical transparency remains constant. So, we can conclude that the O₂ pressures of 300torr give the optimum photovoltaic charecteristics for both samples respectively. Since the constructed device of ZnO/Si heterojunction, the results of the current-voltage (I-V) measurements in the dark for heterojunctions prepared at different substrate temperatures and optimum O₂ pressure are shown in figures 7.

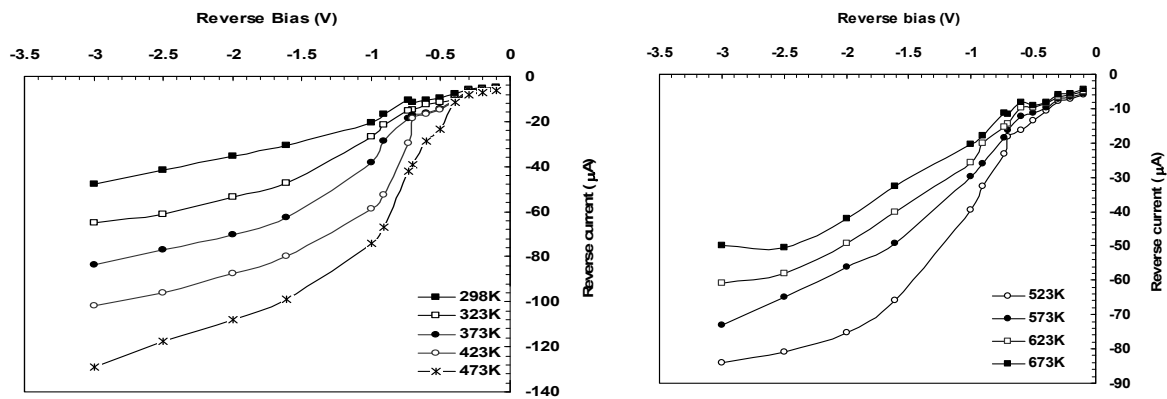


Fig. 7: Dark I-V charecteristics under reverse bias for ZnO\P-Si at different substarte temperatures

These charecterstics are very important to describe the heterojunctin performance and all hetrojunction parameters depending on these charecteristics. In the former curves, the I-V characteristics were given for samples prepared at the optimum conditions under reverse bias. It is clear that the curve contains two regions; the first is the generation region where the reverse current is slightly increased with the applied voltage and this leads to the generation of electron-hole pairs at low bias. In the second region, a significant increase can

be recognized the reverse bias is increased. In this case, the current resulted from the diffusion of minority carriers through the junction. We can also note from this figure the rapid incremental in the reverse current at high reverse voltage, which is probably due to the leakage current arising from the surface layer. The results of I-V characteristics at different substrate temperatures show the tendency of the heterojunctions to have the ideal characteristics with substrate heating up to the optimum temperatures (473K) samples and fall down beyond this temperature. Figures 8 clearly the optimum value of the substrate temperature.

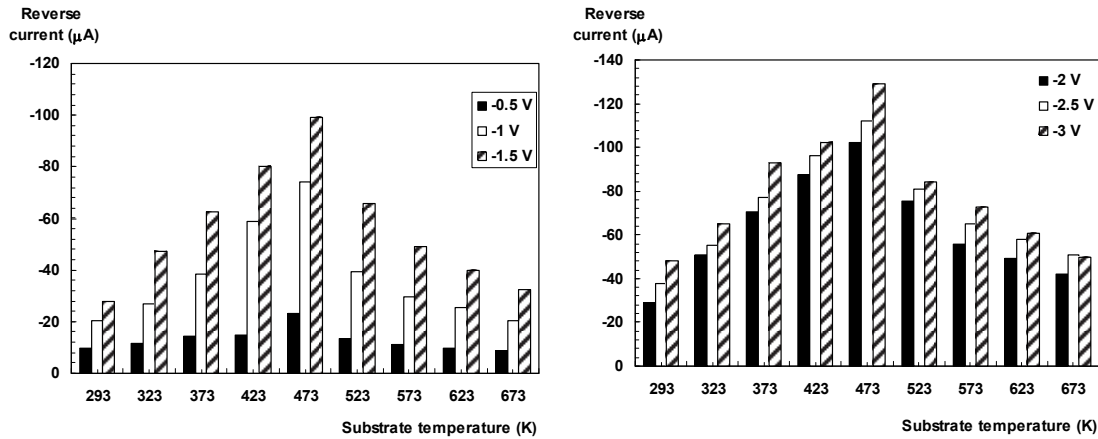


Fig. 8: Comparison between different values of reverse current at different substrate temperatures for ZnO sample

The enhancement of the reverse current is related to the enhancement in the junction structure, which results in reducing the number of defects at semiconductor-insulator-semiconductor interfaces of the two junctions. These defects result from the strain due to crystal structure, lattice parameter and probably a thermal expansion mismatch, which was enhanced when the substrate was heated. In the forward bias, the forward voltage results in reducing the height of the potential barrier, therefore, majority carriers are able to cross the potential barrier much easier than at zero bias, so that the diffusion current becomes greater than the drift current.

The results in figure 9 give the I-V characteristic behavior of the ZnO/P-Si heterojunctions in the forward bias. Two regions are recognized; the first one represents recombination current while the second represents tunneling current.

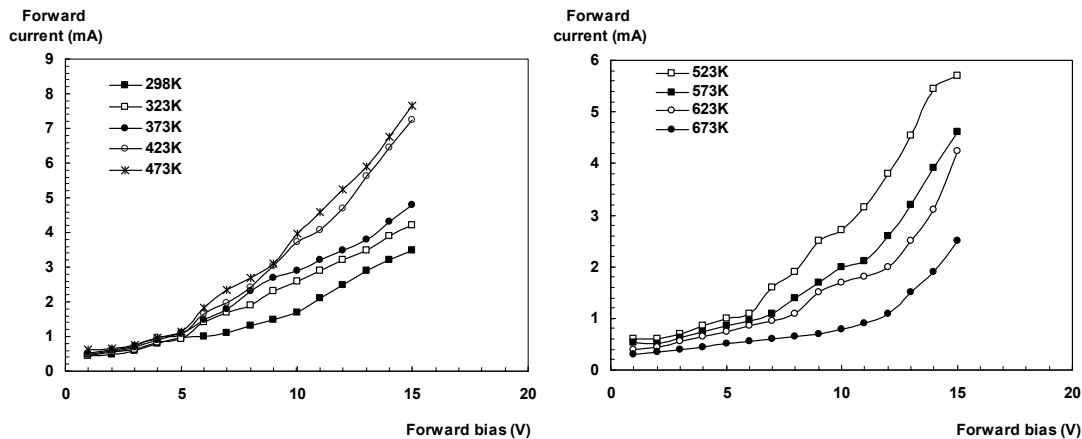


Fig. 9: Comparison between different forward currents for (a) ZnO/Si junctions at different substrate temperatures

Figure 10 displays the comparison between the results obtained at optimum O₂ pressure and different deposition temperatures and different forward voltage for the junctions.

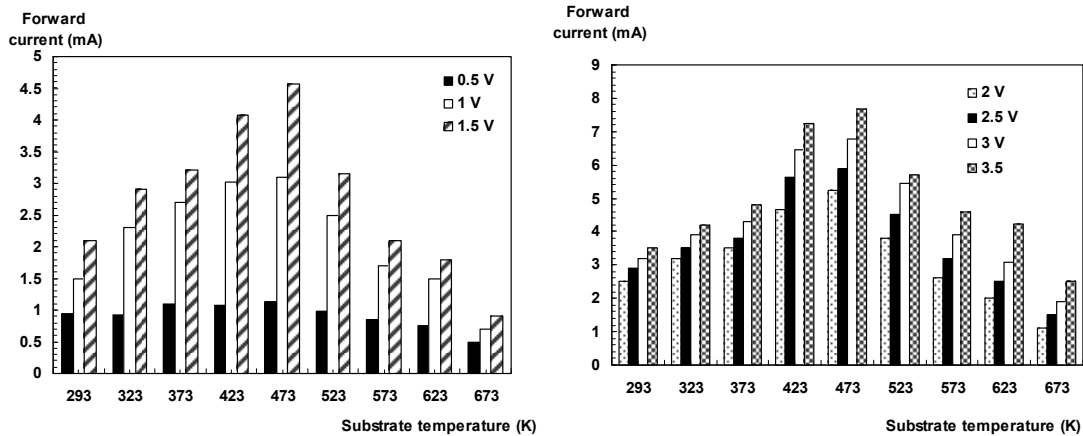


Fig. 10: Comparison between different forward currents at different substrate temperatures for ZnO/Si

Most of the samples were prepared at various deposition temperatures exhibit good rectification behavior and their leakage currents tend to increase with the substrate temperature.

This implies that an interfacial SiO₂ layer between TCO film and Si substrate is probably formed and it becomes thicker as the substrate temperature is increased. The ideality factor of (ZnO/Si) junction at optimum conditions of O₂ pressure and substrate temperature was estimated at the to be 3.78. These values refer to good rectification properties for both prepared junctions. The large value of n (>2) suggests that in this voltage regime, the recombination in these devices occurs primarily in the junction depletion region and/or at the junction interface, these results are consistent with other results reported elsewhere [23,24]. From these results, we can conclude that the best deposition temperatures (T_{sub}) are 473K at which the highest current is obtained and this is attributed to the total transformation of the metal to its oxide as the mismatch being at minimum, hence, the junction has its optimum properties. Also, the suitable substrate temperature results in uniform distribution of the atoms on the sample surface that leads to the optimum junction behavior. The nonuniform distribution with low film thickness at high substrate temperature results in the reduction of the current with the bias voltage. On the other hand, due to the thick interfacial oxide layer, the low substrate temperature causes film thickness to increase, which in turn increases the effect of lattice mismatch and the number of defects, in addition to the effect of dislocation and vacancies that work as trapping centers resulting in lower current. similar result have been investigated for n-Si but they did not match similar good behavior, therefore they were not take into consideration. C-V measurements is one of the most important measurements since it determines different parameters such as built-in potential, junction capacitance and junction type. Figures 11 give the C-V and $1/C^2$ -V measurements for junctions at optimum substrate temperatures and O₂ pressures.

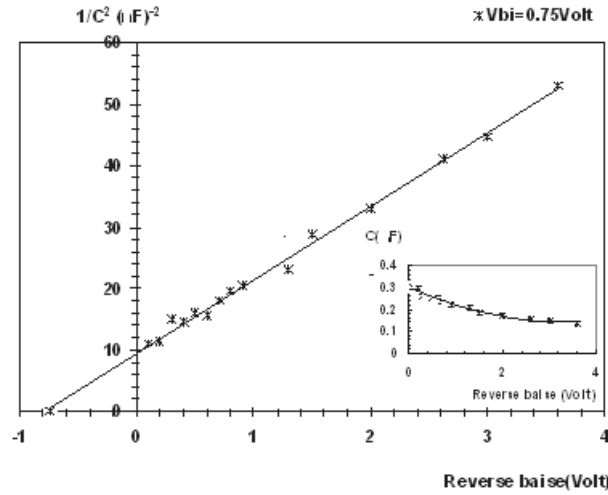


Fig.11: C-V charecteristics for ZnO\Si heterojunction

Results show that the junction capacitance is inversely proportional to the bias voltage for all prepared samples. The reduction in the junction capacitance with increasing bias voltage resulted from the expansion of depletion layer with the built-in potential. The depletion layer capacitance refers to the increment in charge per unit area to the incremental change of the applied voltage. This property gives an indication of the behavior of the charge transition from the donor to the acceptor region, which was found to be “**abrupt**”, which is confirmed by the relation between $1/C^2$ and reverse bias being a straight line. Figure 12 shows the value of the built-in potentials for junction prepared at different substrate temperature and the optimum O_2 pressure.

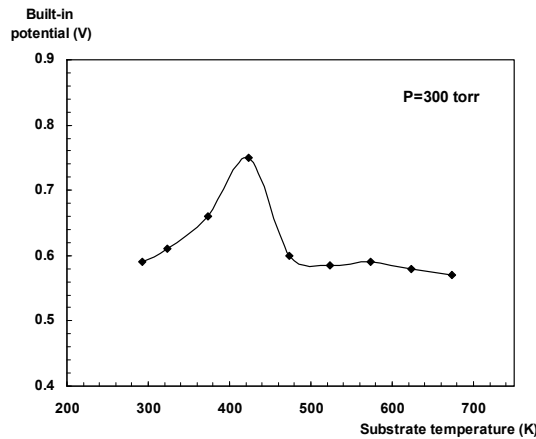


Fig.12: Comparison between different built-in potential for ZnO/Si junctions at different substrate temperatures

These results provide a suitable value of the built-in potential at low temperatures and this value begins to increase up to the optimum substrate temperature (T_{sub}) of 473K for prepared junction.

The value of V_{bi} is expected to depend on the Fermi level position in the conduction band at high carrier concentrations and this explains the relatively large V_{bi} value at low temperatures, where large number of metal atoms does not oxidize and acts as an impurity atom, since in n-type semiconductor Fermi level is proportional to the donor concentration. The spectral responsivity represents the ratio between the output generated current to the incident power and it is very important because it specifies the performance

range of detector. Figure 13 gives the responsivity as a function of wavelength for samples prepared at optimum deposition conditions (O_2 pressure and substrate temperature).

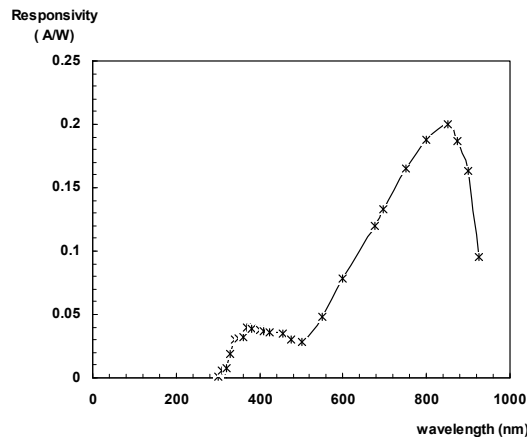


Fig. 13: The spectral responsivity as a function of the incident wavelength at optimum conditions for ZnO/Si samples

In this junctions, we can recognize three different regions on the curve. The first, (short wavelengths) implies a considerable increase in the responsivity and this increase relates to the high absorption coefficient. This leads to lower absorption depth and fast recombination process compared with any other region inside the material and this is called the probability of carrier concentration, which increases with the departure from the surface region, which means rise the responsivity in this region followed by decrease in responsivity value which is related to the large surface recombination processes. In the second region (700-900nm), we observe the highest value of the wavelength-dependent responsivity as these wavelengths are absorbed at the active region of the MIS junction interface (depletion region) and along a distance equal to the diffusion length of minority carriers.

At this region, the generated electron-hole pairs move due to the internal electric field beside the negligible recombination process in this region. The maximum responsivity appears at 800 ± 50 nm despite the fact that this region is far from the cutoff wavelength. This happens in order to coincide with mass action law ^[24,25]. In the third region, (>850nm), the incident light is absorbed within the material where the bulk recombination processes take place, so the carrier concentration probability can exist in this case leading to lower responsivity. Because the ZnO semiconductor has a wide and direct band gap, it could be used to collect high energy photons. This makes this structure of suitable for use as UV detector. Also, the photons of lower energy than UV will be collected at the semiconducting material of the base after being transmitted through the ZnO surface layer. The effect of the substrate heating temperature can be shown in figure 14 for ZnO/Si heterojunctions and the optimum substrate temperature was found to be 473K.

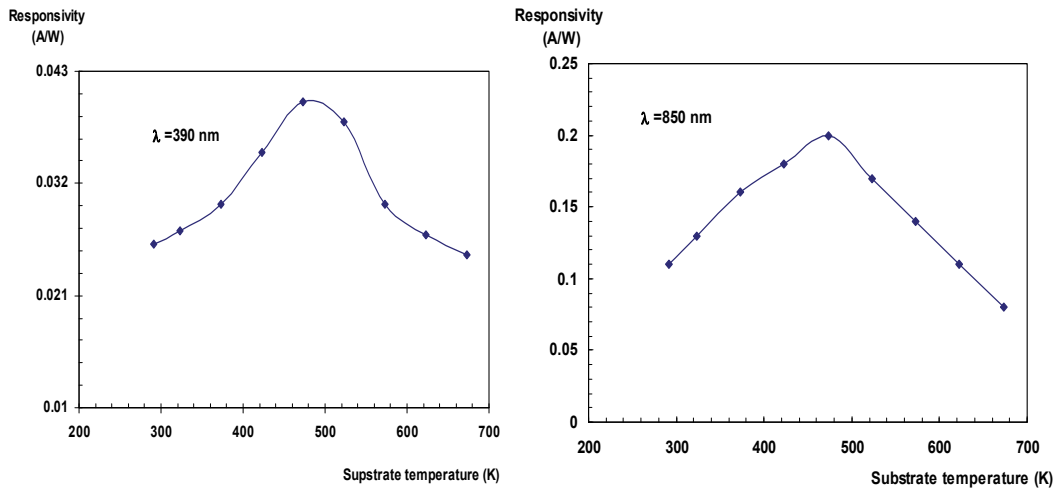


Fig. 14: Responsivity as a function of deposition temperature for ZnO/Si

A slight increase in the responsivity, as the heating temperature is raised up to its optimum value, can be recognized in the last figures. The low responsivity at low substrate temperatures could be attributed to the increase in film thickness, i.e., increase in the structure defects and dislocations, which act as trapping centers that reduce the generated electron-hole pairs at the interface similar result could be shown in other reference[26].

The increase in substrate temperature up to its optimum enhances the junction properties due to the uniformity of the deposited film, which reduces the defects. Also, this enhancement is related to the SiO₂ interfacially layer incorporated in the SIS or more specifically in MIS structure. It can be expected that a thin layer of SiO₂ will be enhanced at the interface during heating process and this oxide layer can strongly affect the device performance. Further increase of the deposition temperature leads to poor responsivity due to two possible reasons; the strain resulting from the deformation of film structure and probably the mismatch in the thermal expansion coefficient, which reduces the photocurrent.

Figure 15 shows the quantum efficiency of the detector as a function of deposition temperature.

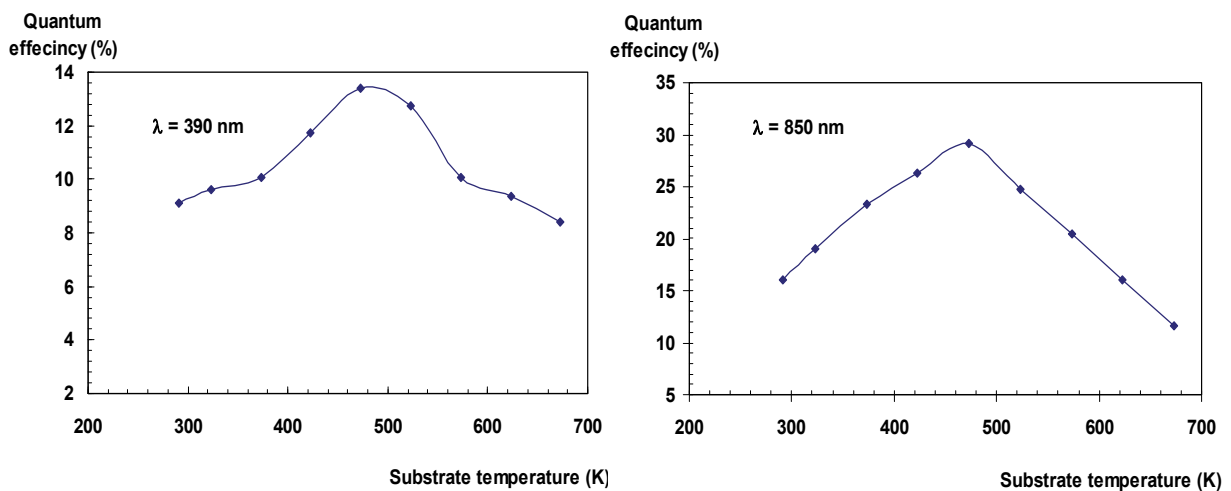


Fig. 15: Quantum efficiency as a function of deposition temperature for ZnO/Si samples

The increase in the photocurrent is attributed to the same reasons of the responsivity. In SIS model, the interfacial layer is taken to be a wide-gap insulator (SiO_2), which acts as a tunneling barrier for carrier transport from one side of the junction to the other. This layer is directly affected by substrate heating during film deposition where the efficiency is slightly enhanced with temperature up to its optimum value and is reduced beyond this value. The highest heating temperature (above 473K) results in deforming the film structure and increasing the insulator layer thickness which decreases the tunneling probability exponentially, and this reduces the photo-current value. The suitable (SiO_2) thickness appearing at the optimum heating temperature greatly enhanced the detector efficiency. The figure of merit of the detectors D^* is defined as the root mean square (r.m.s.) of the signal to noise ratio (SNR) in 1Hz bandwidth per unit r.m.s. incident radiant power per square root of the detector area. The specific detectivity versus wavelength is for (ZnO/Si) devices, directly related to the value of responsivity. So, we can recognize a similarity in the obtained behavior. The most important parameter that specifies the detectivity for a given detector is the noise current (I_n) that is shown in Figure 16 as a function of the substrate temperature.

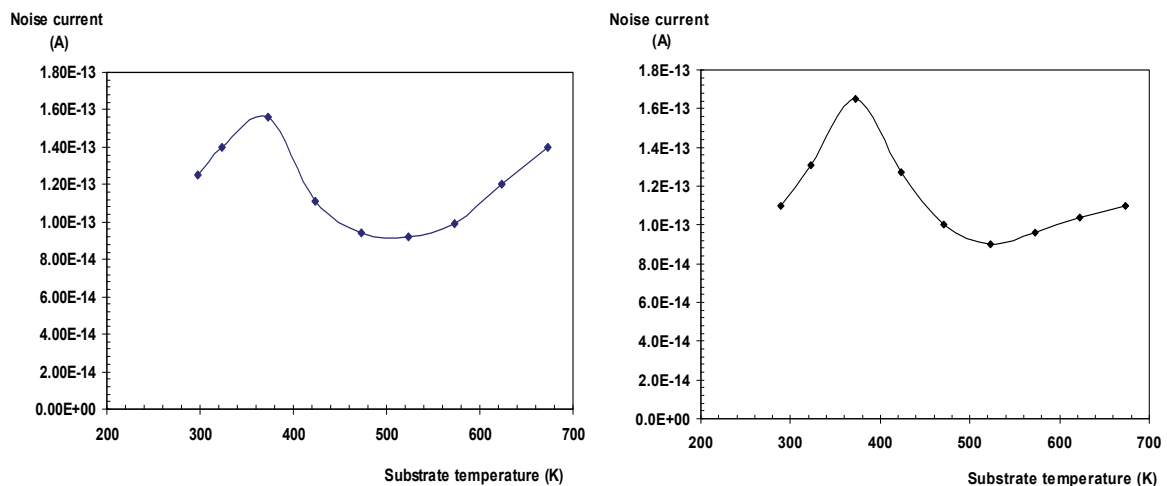


Fig. 16: Noise current as a function of deposition temperature for ZnO/Si samples at optimum O_2 pressure

All detectors are limited to the minimum radiant power that can be detected in the form of noise, which may arise at the detector itself, in the radiant energy to which the detector responds, or in the electronic circuit following the detector. The most common built-in noise within the detector are white noise, Johnson noise and thermal noise, which arises from the random motion of the current carriers within any resistance material. Also, other most important source of noise is the generation-recombination noise that results from the presence of defects acting as trapping centers. The enhancement of noise current with increasing temperature in the last figure ensures the enhancement in the device structure and ensure the reduction in the dislocations and trapping centers with decreasing film thickness especially at the optimum deposition temperature. As shown, the slight increase in noise current at temperature larger than the optimum value, is related to the strain, thermal and lattice mismatches leading to increase in generation-recombination noise current. The reduction in the detectivity (D^*) with substrate temperature, larger than the optimum value is shown in figure 17 and it is directly related to the noise current discussed above.

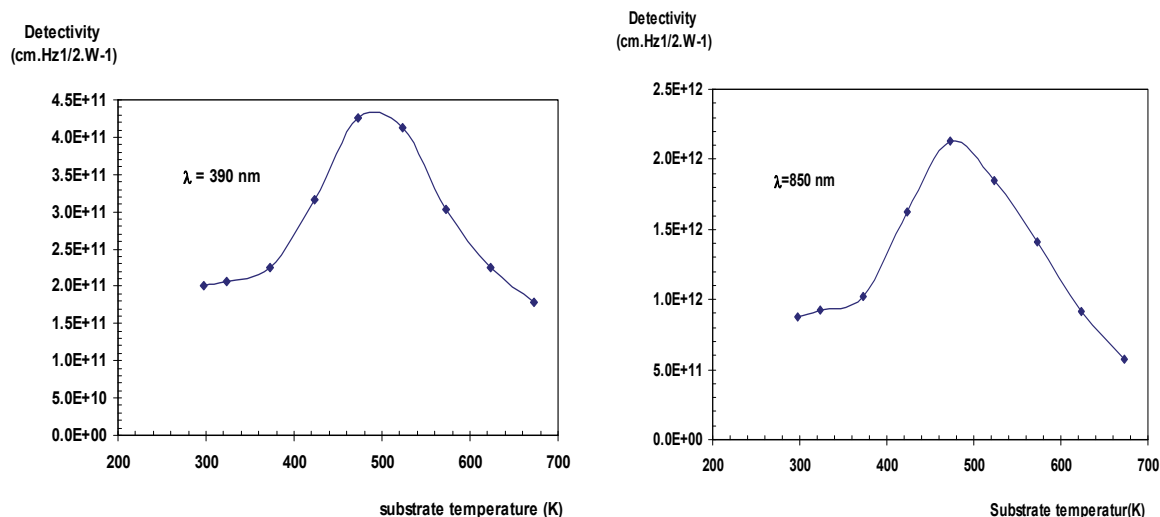


Fig. 17: The specific detectivity (D^*) as a function of deposition temperature for ZnO/Si samples

References

- [1] A.H.Reshak, Int. J. Electrochem. Sci. **9** (2014) 6378
- [2] H.Reshak, Int. J. Electrochem. Sci, **9** (2014) 6352
- [3] K.Ozga *et al.*, Nanotechnology **19** (2008) 185709
- [4] D.Kammler, T. Mason, K. Poepfelmeier, J. Am. Ceram. Soc. **4** (2001) 1004
- [5] R.P.Howson and C.A.bishop, thin solid films **63** (1979) 163
- [6] M. Ortega, G. Santana, A. Morales, Solid state Electron. **44** (2000) 1765
- [7] R. A. Ismail , Bassam G. *et al.*, J Mater Sci: Mater Electron **18** (2007) 397
- [8] R. A. Ismail , Bassam G. Rasheed *et al.*, J Mater Sci: Mater Electron **18** (2007) 1027
- [9] Z. Zhao, D. Moral, C. Ferekides, Thin Solid Films **413** (2002) 203
- [10] M. Dewei, Y. Zhizhen, L. Wang, J. Huang, B. Zhao, Mater. Lett. **58** (2003)128
- [11] M. Yan, M. Lane, C. Kannewurf, R. Chang, Appl. Phys. Lett. **78** (2001) 2342
- [12] Evan T, Salim, Makram A, *et al.*, Int. J. nanoelectronic and Material **6** (2013)121
- [13] J. J. Robbine, Applied physics letters, **183** (19) (2006) 3933
- [14] M. M. Abd El-Raheem, H. M. Ali, *et al.*, Journal of Non-oxide Glasses **2** (2010) 67
- [15] D. Beena, K.J. Lethy, R. Vinodkumar, *et al.*, Solar Energy Materials & Solar Cells **91** (2007) 1438
- [16] A.V. Singh, M. Kumar, R. M. Mehera, J. Indian Inst. Sci. SRP, **81** (2001) 527
- [17] M. Bouderbala *et al.*, Physica **B 403** (2008) 3326
- [18] Reshak, A. H *et al.*, Physica E: Low-dimensional Systems and Nanostructures, **42** (5) (2008) 1769
- [19] Z. Charifi, H. Baaziz and Ali Hussain Reshak, phys. stat. sol. (b) **244** (9) (2007) 3154
- [20] E.T. Salim, Ph.D Thesis, University of Technology , Baghdad, Iraq, (2006)
- [21] J. Trefny and N. Mitra, Thin Solid Films **157** (1988) 7
- [22] .S.choi,J.Y.lee.S.I.M., Jpn.J.Appl.phys.**42** (2003)1560
- [23] Evan T. Salem , Ibrahim R. Agool *et al.*, International Journal of Modern Physics B. **25** (29) (2011) 3863–3869
- [24] Evan T. Salem & Farhan A. Mohamed, Eng. & Tech. Journal, **28** (21) (2010) 6253
- [25] Evan T. Salim , Marwa S. Al Wazny, Eng. & Tech. Journal **32** Part (B) 1 (2014) 33